Bounds on hadronic axions from stellar evolution

Georg G. Raffelt
Institute for Geophysics and Planetary Physics, Lawrence Livermore National Laboratory, Livermore, California 94550 and Astronomy Department, University of California, Berkeley, California 94720

David S. P. Dearborn
Institute for Geophysics and Planetary Physics, Lawrence Livermore National Laboratory, Livermore, California 94550
(Received 20 February 1987)

We consider in detail the effect of the emission of "hadronic" invisible axions (which do not couple to electrons) from the interior of stars on stellar evolution. To this end we calculate plasma emission rates for axions due to the Primakoff process for the full range of conditions encountered in a giant star. Much attention is paid to plasma, degeneracy, and screening effects. We reconsider the solar bound by evolving a 1.0 $M_\odot$ star to solar age and lowering the presolar helium abundance so as to obtain the correct present-day luminosity of the Sun. The previous bound on the axion-photon coupling of $G_9 \lesssim 2.5$ (corresponding to $m_a \lesssim 17$ eV R where R is a model-dependent factor of order unity) is confirmed, where G_9 is the coupling constant G in units of 10^{-9} GeV^{-1}. We then follow the evolution of a $1.3M_\odot$ star from zero age to the top of the giant branch. Helium ignites for all values of G consistent with the solar bound; however, the core mass, surface temperature, and luminosity at the helium flash exceed the standard values. The luminosity at the helium flash is larger than about twice the standard value unless $G_9 \lesssim 0.3$ (corresponding to $m_a \lesssim 2$ eV R), in conflict with observational data, which are statistically weak, however. We find our most stringent limits from the helium-burning lifetime. In the absence of axion cooling we calculate a lifetime of 1.2×10^8 yr which corresponds well with the value 1.5×10^8 yr derived from the number of red giants in the "clump" of the open cluster M67 and with the value 1.3×10^8 yr derived from the number of such stars in the old galactic disk population. We obtain a conservative limit of $G_9 < 0.3$ which, at saturation, results in a helium-burning lifetime an order of magnitude low. We believe that $G_9 \lesssim 0.1$ ($m_a \lesssim 0.7$ eV R) is a reasonably safe limit which, if saturated, leads to a calculated helium-burning lifetime a factor of 2 below the observed value. Our results exclude the recently suggested possibility of detecting cosmic axions through their 2γ decay and probably the possibility of measuring the solar hadronic axion flux which, according to our bounds, must be less than 2×10^{-3} of the solar luminosity. There remains a narrow range of parameters ($0.01 \lesssim G_9 \lesssim 0.1$, $m_a \lesssim 10^{-4}$ eV) in which a recently proposed laboratory experiment might still measure axionlike particles.

I. INTRODUCTION

The issue of *CP* conservation in strong interactions remains unresolved, the most elegant possible solution still being the Peccei-Quinn mechanism.[1] In this approach a global chiral U(1) symmetry is imposed on the fundamental interactions and is effectively used to "rotate away" the unwanted *CP*-violating phase angle $\bar{\Theta}$. This Peccei-Quinn symmetry is spontaneously broken by a vacuum expectation value $v_{\rm PQ}$ of Higgs fields, thereby giving rise to the existence of an (almost) massless, pseudoscalar Goldstone boson: the much-discussed axion.[2] The experimental or observational consequences of the existence of this particle allow one, in principle, to test the validity of the Peccei-Quinn scheme.

The identification of $\sqrt{2}\,v_{\rm PQ}$ with the scale $f_{\rm weak} \approx 250$ GeV at which the $SU_L(2)$ symmetry of weak interactions is spontaneously broken leads to the notion of "standard" axions[3] and a recent variation of this scheme leads to "variant" or "short-lived" axions,[4] all of which appear now to be ruled out by compelling experimental evidence.[5] Therefore, the focus remains on "invisible"-axion models[6] which are characterized by a large value $v_{\rm PQ} \gg f_{\rm weak}$. The requirement that the energy stored in primeval oscillations of the axion field does not "overclose" the Universe leads to the upper bound[7] $v_{\rm PQ} \lesssim 10^{12}$ GeV. If this bound were saturated axions would be the dark matter of the Universe and they would, in particular, constitute the dark halo of our own Galaxy.[8] Experiments[9] to measure this hypothetical galactic axion flux are under way, and first results have been reported.[10] However, the resulting upper bound on the axion-photon coupling (assuming that galactic axions exist) is trivially satisfied in all typical axion models. It will take several years before the issue of galactic axions in the mass range around 10^{-5} eV can be ultimately settled.

Lower bounds on the Peccei-Quinn scale can be obtained from astrophysical arguments. If agreement of the theory of stellar evolution, including the effect of axion cooling, with observational evidence is required, upper bounds on the axion's coupling strength to various particles (electrons, photons, nucleons) can be derived.

These bounds may then be translated into lower bounds on v_{PQ} and on the axion mass m_a. In contrast with the cosmological upper bounds on v_{PQ}, these astrophysical lower bounds strongly depend on details of the specific invisible-axion model, or rather, on details of how the Peccei-Quinn symmetry is implemented.

From a phenomenological point of view invisible-axion models can therefore be subdivided into the classes of "hadronic"[6] and Dine-Fischler-Srednicki-Zhitnitsky-(DFSZ-) type[11] invisible-axion models. The former term generically refers to models in which the axions do not couple to leptons at tree order, the main example being the Kim-Shifman-Vainshtein-Zakharov (KSVZ) model.[12] The coupling to nucleons through a small π^0-η-axion mixing is of similar strength in both types of models. However, in the KSVZ model, axions decouple from light quarks for conditions above the quark-hadron phase transition because, in this model, quarks do not carry Peccei-Quinn charges.

DFSZ-type axions would be emitted from the interior of stars mainly through Compton-type photoconversion processes and through bremsstrahlung processes, in other words, through plasma processes involving electrons. In this case the best bound on the Peccei-Quinn scale is $v_{PQ} \gtrsim 10^9$ GeV, relying on observational evidence of white-dwarf cooling times[13] and on detailed evolutionary calculations which indicate that the occurrence of helium ignition in the post-main-sequence evolution of stars would be suppressed due to excessive axion cooling of their degenerate cores—contrary to compelling observational evidence (Ref. 14, to be referred to as paper I).

For hadronic axions one has to rely on processes involving the two-photon coupling of axions, notably on the Primakoff effect (Fig. 1). One of us has recently shown (Ref. 15, to be referred to as paper II) that plasma effects, and in particular Debye-Hückel screening of electric charges, substantially reduce the emission rates to values much below those previously considered. Therefore, all bounds on hadronic axions previously published, including the ones based on the helium-ignition argument (paper I) are unduly restrictive. Then the only available bound on hadronic axions from stellar evolution is based on an argument involving the solar age (paper II).

We write the effective Lagrangian density which describes the coupling of axions to photons as

$$\mathcal{L}_{a\gamma\gamma} = -\frac{G}{4} F_{\mu\nu}\tilde{F}^{\mu\nu} a = G\mathbf{E}\cdot\mathbf{B}a \ , \tag{1}$$

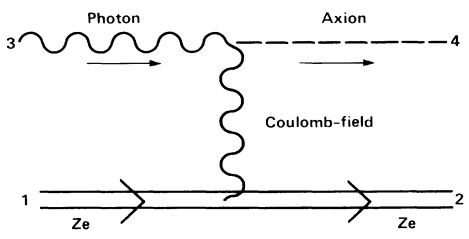

FIG. 1. Primakoff conversion of a photon into an axion in the Coulomb field of a particle of charge Ze.

with the electromagnetic field-strength tensor F, its dual $\tilde{F}$, the axion field a, and a coupling constant G of dimension (energy)$^{-1}$. Then the solar bound of paper II is

$$G \lesssim 2.4\times 10^{-9}\ \text{GeV}^{-1} \ . \tag{2}$$

We shall frequently use the notation $G_9 = G$ in units of 10^{-9} GeV^{-1}. The axion mass is given as[6]

$$m_a = 6.9\ \text{eV}\, R G_9 \ , \tag{3}$$

where, in a large class of grand unified theories, $R=1$. Then the solar bound corresponds to $m_a \lesssim 17\ \text{eV}\, R$.

Most recently it has been pointed out[16] that hadronic axions slightly below the solar bound would have been so abundantly produced in the early Universe that their decay $a \rightarrow 2\gamma$ could produce an observable signal, although their contribution to the overall cosmic mass density would still be entirely negligible. In the relevant parameter range, the dominant primordial production is a thermal mechanism involving the Primakoff amplitude. Relic axions would be detectable unless $m_a \lesssim 2$–5 eV where $R=1$ has been assumed.

It is then very interesting to ask whether other astrophysical arguments besides the solar age restriction yield significant bounds on hadronic axions. An obvious possibility is the consideration of axion emission from the compact stars which are believed to form in certain supernova explosions and which are detectable, in many cases, as pulsars. Usually these objects are identified with neutron stars, and since hadronic and DFSZ-type axions couple to nucleons, they would be abundantly emitted through bremsstrahlung processes in nucleon-nucleon collisions[17,18] in the interior of these stars. Considering the cooling times of neutron stars it has been shown[19] that for $m_a \gtrsim 10^{-2}$–10^{-3} eV R the present-day surface temperature of several young neutron stars would be too low to be compatible with Einstein-observatory measurements if these results are interpreted as *thermal* x-ray signals from the neutron-star surfaces.

It has recently been claimed that axions emerging from pulsars might be detectable through their conversion into photons in the magnetosphere of these objects.[20] It was later recognized,[21] however, that the relevant conversion rate sensitively depends on the photon index of refraction in strong magnetic fields such that the axion-photon conversion is suppressed in the relevant parameter range. Therefore, one has to rely, indeed, on measurements of the surface temperature of pulsars in order to gain observational insight into the question of axion cooling of these compact stars. Whether or not the Einstein measurements can be identified with thermal surface emission can be resolved only by future x-ray satellites which will hopefully be able to establish the blackbody nature of the relevant sources in supernova remnants.[19]

Even then, however, there remain unresolved issues concerning the inner structure of these stars which are very important for the calculation of the expected axion flux. If the nucleons are in a state of superfluidity, bremsstrahlung emission would be strongly suppressed. Furthermore, even the identification of pulsars with neutron stars is uncertain. It has recently been recognized[22]

that the ground state of bulk nuclear matter may possibly be "strange-quark matter," and that pulsars may possibly be strange matter stars, or shorter, strange stars.[23] From an observational point of view, these two cases are hardly distinguishable, and it is not very likely that the understanding of QCD will soon improve quantitatively to a precision where this issue could be resolved on the basis of theoretical calculations.

Axion emission from strange stars would differ substantially from that of neutron stars. DFSZ axions would be emitted mainly through bremsstrahlung emission in quark-quark collisions. In some hadronic axion models, in contrast, axions decouple from quarks for conditions beyond the QCD phase transition. Therefore, in these models, axions would couple only to photons and gluons for conditions as encountered in the interior of a strange star. Photon- and gluon-conversion reactions would be suppressed because the respective plasma frequencies would far exceed the temperature. Therefore, the dominant emission process would be the "electro-Primakoff effect"[24] involving intermediate photons or gluons. Although this emission rate could be very large, a reliable calculation requires detailed considerations of correlation effects and is far beyond the scope of our present discussion.

In the presence of these uncertainties it remains worthwhile to study what can be learned about hadronic axions from evolutionary calculations of main-sequence and giant stars where well-established input physics in connection with presently available observational data can be used. It appears obvious that one should be able to do better than is possible with the solar age argument of paper II. We mention that the comparison in paper II of the axion emission rate with a typical nuclear-energy-generation rate of helium-burning stars shows that axion cooling would be an important effect unless $G_9 \lesssim 0.1$, but we emphasize that this does not constitute a bound on G as long as the effect of axion cooling has not been related to observational data. It indicates, however, that it may be reasonable to expect that, following the methods of paper I, helium ignition would be suppressed in the post-main-sequence evolution of stars for values of G which exceed this number.

In an attempt to confirm this proposition we have extended the calculation of the axion emission rates of paper II to a regime of strong electron degeneracy as is encountered in the core of red-giant stars. Using these emission rates we have numerically followed the evolution of a $1.3M_\odot$ star for various values of G, mainly in order to compare the theoretical Hertzsprung-Russell diagram thus obtained with observational data concerning the open star cluster $M67$ for which very detailed photometric measurements exist.[25,26] We mention that we have to focus on stars with masses below about $2.2M_\odot$ because beyond this value the transition to helium burning is relatively smooth because of the absence of a strongly degenerate core in their post-main-sequence evolution. Therefore, the well-studied cluster $M67$ which contains Population I stars (i.e., stars of the most recent generation) of very similar chemical composition as the Sun,[26] is an ideal candidate for our purposes.

It turned out, however, that contrary to our initial expectation *the helium flash did occur in the whole range of values for the axion-photon coupling compatible with the solar age argument,* i.e., for $G_9 \lesssim 2.5$. It occurred, however, at core masses, surface temperatures, and surface luminosities exceeding the standard values by G-dependent amounts. Therefore, the increased surface luminosity at the helium flash can be used to set bounds on axions if it is compared with the observed maximum luminosity at the top of the giant branch in low-mass stellar clusters.

Since helium does ignite in all cases of interest, we also consider the helium-burning phase with the inclusion of axion cooling effects. The dramatic reduction of the time spent in this phase can be translated into a reduction in the number of stars expected in the "clump" of giants which is observed in all open clusters at an almost fixed location in the color-magnitude diagram.[27–29] Specifically for

$$G_9 \lesssim 0.1 \ , \tag{4}$$

corresponding, with Eq. (3), to

$$m_a \lesssim 0.7 \text{ eV} R \ , \tag{5}$$

this number of stars would be reduced by more than about a factor of 2. In view of the impressive agreement between the observationally inferred helium-burning lifetime and stellar structure calculations in the absence of axion cooling,[27,28,30] such a reduction appears to be unacceptable, rendering these numbers reasonably safe bounds on the axion properties. For $G_9 = 0.3$ the relevant reduction would be about an order of magnitude such that the clump of giants would be entirely unobservable in most or all open clusters. Therefore, $G_9 < 0.3$ would be an overly conservative, but certainly absolutely safe bound.

The actual occurrence of the helium flash in this scenario is a very important result for the general method of using stellar evolution as a probe for particle physics. Since the helium ignition argument of paper I offers the most stringent bounds on the properties of such particles as Majorons which may have been detected in a recent $\beta\beta$-decay experiment,[31] it is important to properly understand this approach so that the results and conclusions can be relied upon—ideally with the same degree of confidence as one can trust in laboratory measurements.

The occurrence of the helium flash in our case then specifically indicates that it is not sufficient to thermally isolate the inner core of a giant star from the hydrogen-burning shell in order to suppress the helium flash. The exotic cooling mechanism under consideration must also be efficient *within* the degenerate core such that gravitational energy release—a local energy source—is sufficiently balanced. This means that much attention must be paid to the plasma energy-loss rates under such extreme conditions; it is not sufficient to focus on the much less exotic regime of the hydrogen-burning shell and the region immediately behind it.

In paper I no effort has been made to construct de-

tailed energy-loss rates for the inner core of the star. In the light of our present results it is then not entirely obvious that the bounds on axions, familons, and Majorons derived in this previous study are as reliable as was originally thought. We emphasize, however, that the dominant emission process in the degenerate core for the cases discussed in paper I is electronic bremsstrahlung. It would not suffer from the $e^{-\omega_{\rm pl}/T}$ suppression at high densities which is characteristic of photoconversion (or rather plasmon conversion) processes—contrary to the opposite statement implicit in Eq. (3) of paper I. It would suffer, however, from a substantial reduction because of electron degeneracy effects when the temperature dependence of the bremsstrahlung rates, which dominate in the core, would be[13,17] as T^4, in contrast with $T^{2.5}$ for the nondegenerate regime.[15,32] More specifically, the assumed bremsstrahlung emissivity of paper I is

$$\epsilon_{\text{paper I}}=4.2\times10^2\ \text{erg g}^{-1}\,\text{s}^{-1}\alpha_{26}\rho_6 T_8^{2.5}e^{-\omega_{\rm pl}/T}\ ,$$

where α_{26} is the axionic fine-structure constant, $\alpha_a=g^2/4\pi$ in units of 10^{-26}, $\rho_6=\rho/10^6$ g cm^{-3}, $T_8=T/10^8$ K, and $\omega_{\rm pl}$ is the plasma frequency given as $\omega_{\rm pl}/T=2.4\rho_6^{0.5}/T_8$ for a helium plasma. The correct emissivity for a helium plasma is

$$\epsilon_b=F(\pi^2/15)\alpha^2\alpha_a T^4 m_e^{-2}m_u^{-1}\ ,$$

where m_u is the atomic mass unit and F is a numerical factor of order unity which includes the effect of ion-ion correlations.[33] Hence paper I overestimates the emission rate by a factor

$$r\equiv\epsilon_{\text{paper I}}/\epsilon_b$$
$$=(38.7/F)\rho_6 T_8^{-1.5}\exp(-2.4\rho_6^{0.5}/T_8)\ .$$

The precise value for F has not been calculated for the relevant case of a helium plasma. However, for conditions of a red-giant core before helium flash ($\rho_6\approx1$ and $T_8\approx1$) $F\approx1.5$ appears to be a good estimate.[33] Then $r\approx2.3$, and we conclude that the bounds on the axion mass and on symmetry-breaking scales given in paper I are possibly too restrictive by a factor not larger than about 1.5.

Returning to the case of hadronic axions we proceed to present our results in detail by revisiting the solar bound on these particles in Sec. II. We specifically discuss the connection between the inferred presolar helium abundance and the effect of axion cooling. In Sec. III we calculate the Primakoff-emission rate for the whole range of conditions encountered in the interior of a giant star, paying particular attention to plasma, degeneracy, and screening effects. In Sec. IV we follow the evolution of a $1.3M_\odot$ star from zero age to the helium flash for various values of the axion-photon coupling strength G. We establish, in particular, the dependence on G of the core mass, surface temperature, and surface luminosity at the helium flash. In Sec. V we follow the helium-burning phase of these stars, and establish their helium-burning lifetime. In connection with observational data on the relative abundance of helium burning stars, these results are used to set new bounds on G. We summarize the results of this work in Sec. VI and discuss some consequences concerning several schemes proposed to detect axions.

II. SOLAR BOUNDS ON HADRONIC AXIONS AND THE PRESOLAR HELIUM ABUNDANCE

In paper II the axion-emission rate, due to the Primakoff process (Fig. 1) from a nondegenerate, nonrelativistic plasma, has been calculated with much attention to screening effects of electric charges in such an environment. Then the axion luminosity L_a from the Sun was calculated from a standard solar model under the assumption that axion emission was only a minor perturbation. The requirement that L_a does not exceed the surface photon luminosity L_s was used to derive the bound Eq. (2), and this requirement was justified by the observation that otherwise the Sun would have turned off the main sequence before its observed age of $t_\odot=4.5\times10^9$ yr.

This argument, as presented in paper II, is somewhat rough because for $L_a\approx L_s$ axion emission is a strong effect and the structure of the Sun would substantially differ from a standard model. Therefore, we presently investigate this argument in more detail by numerically considering the evolution of $1.0M_\odot$ star from zero age to $t_\odot$ where we include the effect of axion emission as calculated in paper II. To this end we have used the same stellar structure code that has been described in paper I. We mention that the way we use this code is well adapted to follow the structure of a star from zero age up the giant branch to the helium flash and beyond in an efficient and economical way. We used a mesh of 150 points to solve the differential equations, and the zoning was kept variable in order to accommodate such singular conditions as thin-shell hydrogen burning. This procedure, however, is not well suited to model the Sun in all its fine points, and it would be entirely inadequate to study such questions as the solar-neutrino puzzle. In the present case, however, we are only interested in gross changes brought about by substantial axion cooling, and, therefore, it appeared acceptable to use the same numerical procedure as in the subsequent sections of this paper.

We consider a solar model acceptable and consistent if it reproduces the observed luminosity $L_\odot=3.86\times10^{33}$ erg/s at the age $t_\odot=4.5\times10^9$ yr. We use a metallicity of $Z=0.02$. No attempt has been made to model the convective surface layers such as to reproduce the solar radius (or surface temperature). No attention has been paid to the solar-neutrino spectrum, because, in spite of the dramatic changes brought about by a substantial modification of the standard solar model, it is well conceivable that these changes could be compensated for by neutrino oscillation phenomena[34] such that present and future measurements of the solar-neutrino flux cannot be used to constrain properties of the solar interior in a simple and straightforward fashion.

The only parameter which we vary in order to achieve consistency of our models with the present Sun is the

presolar helium abundance. This number cannot be determined with any precision from a spectroscopic analysis of the solar photosphere because of the "invisibility" of helium at the given surface temperature. Therefore, the presolar hydrogen mass fraction X (or the helium mass fraction $Y=1-X-Z$) represents the most uncertain input parameter of solar structure calculations. In practice it is therefore an *output* result of such calculations and is chosen to achieve consistency with all other input information. Older calculations typically found[35] $Y\approx 0.27$, while detailed solar modeling in the context of the solar-neutrino puzzle[36] leads to $Y=0.25\pm 0.01$. Recently other authors have disagreed with this number and find[37] $Y=0.285$ instead.

In Table I we display our results for some global parameters of a $1M_\odot$ star at age $t_\odot$ with various values for X and the axion-photon coupling G. In the absence of axion cooling ($G=0$) we find that $X=0.706$ ($Y=0.274$) yields an acceptable solar model, but this value is not claimed to be equally significant as the quoted results from fine-tuned solar models. One of us and G. Fuller[38] have recently developed a version of our code with a much increased number of zones which reproduces the solar-neutrino spectrum of Ref. 36 with $X\approx 0.75$.

For a fixed value of X the effect of axion cooling leads, somewhat counterintuitively, to an *increase* of the present-day luminosity of the Sun. This effect can be compensated by an *increase* of X, i.e., by an *increase* of the presolar amount of hydrogen fuel. In the last column of Table I we give the values $\Delta X=-\Delta Y$ necessary to obtain the present solar luminosity. We obtain these values from an interpolation between the entries of Table I. We believe that our results for ΔX are much more significant than our absolute values for X; they should remain valid for the solar models of other authors.

For $G_9=2.5$ which just saturates the bound Eq. (2) an increase of X by 0.05 is sufficient to make our model "acceptable." We note that at the present time the axion luminosity would be about twice as large as the photon emission, and hydrogen is almost exhausted in the center. Although such a state of the present-day Sun appears to be just barely acceptable, we find it difficult to exclude it by any simple argument. In particular, the required low presolar helium abundance, although certainly somewhat extreme, is difficult to strictly exclude observationally. This applies even more to the case $G_9=2.0$ where $\Delta X=0.03$ suffices to achieve a consistent Sun. For $G_9=3.0$, on the other side, it appears entirely impossible to construct an acceptable Sun by variation of X.

The derived presolar helium abundance can be compared with the observational abundance of metal-poor nebulae and to values obtained from models of the chemical evolution of the Galaxy in conjunction with the primeval helium abundance as obtained from big-bang nucleosynthesis calculations (see the discussion in Ref. 37). Although these numbers are roughly consistent, a discrepancy of a few 0.01 cannot be easily excluded. A value of the presolar helium abundance as large as[37] $Y=0.285$, however, would possibly present a problem in the sense that it is too large to be easily reconciled with the observational evidence.[37] Recently it has been claimed,[39] furthermore, that the observed helium abundances of extragalactic nebulae have been systematically overestimated due to problems concerning the translation of observed spectral line strengths into chemical abundance ratios. Therefore, the possible problem of too large a value for Y from solar evolution calculations would be even worse than discussed in Ref. 37. Hence a decrease of Y below its standard value because of axion cooling (or other effects) cannot be easily

TABLE I. Numerical results for a $1.0M_\odot$ star. It was evolved from zero age to $t_\odot=4.5\times 10^9$ yr with a metallicity of $Z=0.02$ for the tabulated values X of the presolar hydrogen abundance and of the axion-photon coupling constant G_9. The increase ΔX above our standard value $X=0.706$ is necessary to reach $L_s=L_\odot$ at $t=t_\odot$ which was obtained from interpolating the tabulated results. L_s is the surface luminosity in units of $L_\odot$, L_a is the axion luminosity in $L_\odot$, T_s is the surface temperature in degrees Kelvin, and T_c is the temperature at the center. For $G_9=3.0$ it appears that the Sun cannot be made consistent by variation of X.

G_9	X	$\log_{10}L_s$	$\log_{10}L_a$	$\log_{10}T_s$	$\log_{10}T_c$	X_c	ΔX
0.0	0.70	0.023		3.765	7.196	0.342	
	0.73	−0.090		3.750	7.159	0.441	
1.0	0.70	0.056	−0.666	3.769	7.232	0.234	0.008
	0.73	−0.060	−0.819	3.755	7.182	0.386	
1.5	0.70	0.089	−0.204	3.769	7.275	0.214	0.018
	0.75	−0.098	−0.467	3.751	7.186	0.377	
2.0	0.70	0.200	0.299	3.766	7.336	0.001	0.033
	0.73	0.032	0.061	3.761	7.283	0.225	
	0.75	−0.040	−0.044	3.758	7.253	0.270	
2.5	0.70		Turns off main sequence at 3.5×10^9 yr				0.050
	0.75	0.021	0.308	3.748	7.314	0.136	
	0.80	−0.168	0.036	3.744	7.229	0.273	
3.0	0.78		Turns off main sequence at 4.4×10^9 yr				
	0.79	−0.030	0.514	3.729	7.340	0.073	
	0.80	−0.077	0.464	3.736	7.311	0.180	

excluded and, on the contrary, would perhaps be quite desirable and attractive.

We conclude that the solar bound Eq. (2) appears to be firm, but that its near saturation cannot be easily excluded from the resulting decrease of the inferred presolar helium abundance. The changes in the solar-neutrino spectrum could, perhaps, be reconciled with present and future experimental data by neutrino oscillation phenomena. Therefore, we confirm the solar bound of paper II, but we are unable to easily improve on it in any significant way. We then proceed to consider the evolution of stars beyond their main-sequence phase.

III. PRIMAKOFF EMISSION OF AXIONS FROM STELLAR PLASMAS

The Primakoff emission rates of paper II have to be extended to a regime of extreme electron degeneracy, which also implies a large value for the plasma frequency, in order to use them for an evolutionary calculation of giant stars. Prior to helium ignition typical conditions for a $1.3M_{\odot}$ star range from ρ near 10^6 g cm^{-3} at T near 10^8 K in the center of the star to ρ around 1 g cm^{-3} at T around 10^7 K in the hydrogen-burning shell, i.e., from strongly degenerate to entirely nondegenerate conditions (see Fig. 2). We remain, however, in the realm of nonrelativistic physics. We emphasize that the detailed calculations of Primakoff emission rates of Ref. 18, which appeared shortly after the publication of paper II, do not take screening effects into account and, consequently, cannot be used for our present purposes.

Since many of the approximations used in paper II do not apply in the present context we begin our discussion with the basic expression for the energy-loss rate ϵ^* per unit volume (in erg cm^{-3} s^{-1}) because of the Primakoff effect (Fig. 1) on targets of charge Ze ($\hbar=c=k_B=1$):

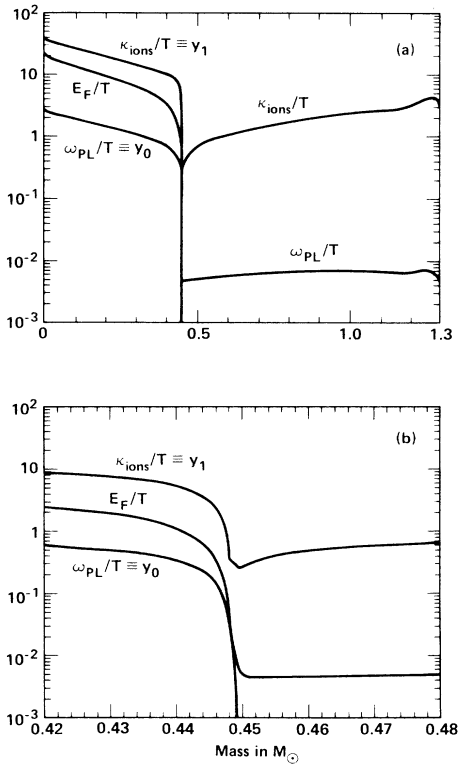

FIG. 2. Plasma frequency $\omega_{\rm pl}$, ionic Debye-Hückel scale $\kappa_{\rm ions}$, and Fermi energy E_F in units of the local temperature in a red giant just prior to helium flash for the case with no axions. (a) is an overview over the whole star; (b) shows only the region near the core boundary, i.e., at the hydrogen-burning shell. Other internal properties of the same star are shown in Fig. 7.

$$\epsilon^* = \int (2\pi)^4\delta^4(k_1-k_2+k_3-k_4)\omega_4 \left[\prod_{j=1}^{4}\frac{1}{2\omega_j}\right] \sum_{\epsilon} |\mathcal{M}_{fi}|^2 S(\Delta) \frac{n_1 d^3\mathbf{k}_1}{(2\pi)^3}\frac{(1-n_2)d^3\mathbf{k}_2}{(2\pi)^3}\frac{n_3 d^3\mathbf{k}_3}{(2\pi)^3}\frac{(1+n_4)d^3\mathbf{k}_4}{(2\pi)^3}\,, \tag{6}$$

where the indices 1 and 2 refer to the ingoing and outgoing target particle, respectively; 3 refers to the (ingoing) photon and 4 to the (outgoing) axion. The sum is extended over photon polarizations. Δ is the momentum transfer in the reaction, and S is the dynamic structure factor[40] which accounts for the spatial correlation of the targets and hence for screening effects in a plasma. n_1 is the relevant occupation number in phase space for the targets, and $1-n_2$ accounts for Pauli blocking of final states in the case of degenerate electrons as targets; for nuclei we use $n_2=0$. n_3 is the relevant blackbody photon occupation number. We shall always neglect n_4 because stimulation effects will not be important in the present context.[41]

In the rest frame of the target and neglecting the energy transfer in the Primakoff reaction we find

$$\sum_{\epsilon} |\mathcal{M}_{fi}|^2 = (ZeG)^2(2m_t)\frac{|\mathbf{k}_3\times\mathbf{k}_4|^2}{|\Delta|^4}\,, \tag{7}$$

where now $\Delta=\mathbf{k}_4-\mathbf{k}_3$ is the three-momentum transfer, and consequently S is now the static structure factor, or effective form factor squared (paper II), of the charged targets. m_t is the target mass which now equals ω_1 and ω_2. Furthermore the axion and photon energies are equal so that

$$\epsilon^* = \frac{(ZeG)^2}{32\pi^4}N_{\rm eff}\int \frac{\omega_3}{e^{\omega_3/T}-1}\frac{|\mathbf{k}_3\times\mathbf{k}_4|^2}{|\Delta|^4}S(\Delta)d^3\mathbf{k}_3\,, \tag{8}$$

where for nuclei and nondegenerate electrons $N_{\rm eff}$ is the relevant number density. For degenerate, nonrelativistic electrons it is the electron number density reduced by the factor

$$R_{\rm deg} = \int_0^\infty \frac{x^2 e^{x^2-\eta}dx}{(e^{x^2-\eta}+1)^2} \Big/ \int_0^\infty \frac{x^2 dx}{e^{x^2-\eta}+1}\,, \tag{9}$$

where η is the chemical potential in units of the temperature. For strong degeneracy $\eta = p_F^2/2m_eT$.

For nondegenerate electrons, when all targets can be treated as classical sources of a static Coulomb field, the static ion structure factor can be approximated to lowest order by the Debye-Hückel expression[40]

$$S(\Delta) = \frac{|\Delta|^2}{\kappa_{nd}^2 + |\Delta|^2} , \tag{10}$$

where κ_{nd} is the inverse Debye-Hückel radius for nondegenerate conditions:

$$\kappa_{nd}^2 = \frac{4\pi\alpha}{T} \sum_j Z_j^2 N_j , \tag{11}$$

with the number density N_j of the target species j with charge $Z_j e$ (for electrons $Z_e = -1$). Overall charge neutrality implies $\sum_j Z_j N_j = 0$.

In the present context axions can be considered to be effectively massless and hence $|\mathbf{k}_4| = \omega_4 = \omega_3$ while for photons $|\mathbf{k}_3| = \sqrt{\omega_3^2 - \omega_{pl}^2}$, where the plasma frequency is

$$\omega_{pl}^2 = 4\pi\alpha N_e/m_e , \tag{12}$$

with the electron number density N_e and electron mass m_e.

Then we find with $y = \omega_3/T$, $y_0 = \omega_{pl}/T$, $y_1 = \kappa_{nd}/T$, and $x = \cos(\mathbf{k}_3, \mathbf{k}_4)$ the following result for the axion emission rate per unit mass $\epsilon = \epsilon^*/\rho$ (in erg g^{-1}s^{-1}), where we have summed over all target species:

$$\epsilon_{nd} = \frac{\alpha G^2}{4\pi} \frac{T^4}{\rho} \left[\sum_j Z_j^2 N_j \right] f(y_0, y_1) , \tag{13}$$

where

$$f(y_0, y_1) = \frac{1}{4\pi} \int_{y_0}^{\infty} dy \frac{y^2 (y^2 - y_0^2)^{1/2}}{e^y - 1} I(y, y_0, y_1) \tag{14}$$

and

$$I = \int_{-1}^{+1} dx \frac{1 - x^2}{(r - x)(r + s - x)} , \tag{15}$$

with

$$r = (2y^2 - y_0^2)/2y(y^2 - y_0^2)^{1/2} ,$$
$$s = y_1^2/2y(y^2 - y_0^2)^{1/2} . \tag{16}$$

Function f is defined as in paper II; however, it includes now the dependence on the plasma frequency and is therefore now a function of two variables. In the present context we may not neglect the plasma frequency because in the core of giant stars ω_{pl} may well exceed the temperature T as is illustrated in Fig. 2. For the integral I we find

$$I = \frac{r^2 - 1}{s} \ln\left[\frac{r - 1}{r + 1}\right] + \frac{(r + s)^2 - 1}{s} \ln\left[\frac{s + r + 1}{s + r - 1}\right] - 2 . \tag{17}$$

The case discussed in paper II where the plasma frequency has been neglected corresponds to $r \to 1$ so that

$$I \to 2(1 + s/2)\ln(1 + 2/s) - 2 , \tag{18}$$

which reproduces the result of paper II with the notation $s \equiv 2\xi^2$. Another limiting case which turns out to be of much interest occurs for $s \gg 1$ when

$$I \to 2r/s . \tag{19}$$

The remaining quadrature has to be performed numerically. In order to save computation time in a stellar evolution code it is therefore necessary to use a tabulated form of f. To this end we have used the parametrization

$$f(y_0, y_1) = \frac{100}{1 + y_1^2} \frac{1 + y_0^2}{1 + e^{y_0}} g(y_0, y_1) , \tag{20}$$

where g is now a slowly varying function for which numerical values are tabulated in Table II. In our stellar evolution code we have then interpolated between these tabulated numbers.

The procedure adopted so far is valid only for nondegenerate electrons. In the general case of arbitrary degeneracy, it is very difficult to determine the exact form of the structure function $S(\Delta)$ even in the static limit. It appears reasonable to assume, however, that little

TABLE II. Numerical values for the function $g(y_0, y_1)$. Note that the values for $y_1 < y_0$ in the upper right part of the Table are never needed in practice because $\kappa > \omega_{pl}$ always (see Fig. 2).

	$\log_{10}(y_0)$					
$\log_{10}(y_1)$	−1.0	−0.5	0.0	0.5	1.0	1.5
−2.0	0.167	0.121	0.060	0.019	0.007	0.000
−1.5	0.164	0.121	0.060	0.019	0.007	0.003
−1.0	0.147	0.118	0.060	0.019	0.007	0.003
−0.5	0.118	0.109	0.062	0.021	0.008	0.004
0.0	0.126	0.125	0.085	0.034	0.014	0.006
0.5	0.281	0.285	0.216	0.116	0.070	0.035
1.0	0.591	0.603	0.472	0.304	0.361	0.292
1.5	0.770	0.786	0.595	0.416	0.758	1.598
2.0	0.808	0.831	0.680	0.493	1.232	3.045
2.5	0.809	0.833	0.685	0.524	1.608	14.47

correlation between electrons and nuclei exists. From the point of view of the nuclei (or ions) the degenerate electron sea is a "stiff background" which cannot be easily polarized. Therefore, electrons do not contribute to the screening of nuclear charges which then will be screened only by the relative displacement of other ions against the uniform electron background. Therefore, in this regime, ion targets should be treated with exactly the same procedure as above, but dropping electrons from all summations:

$$\epsilon_{\rm ions}=\frac{\alpha G^2}{4\pi}\frac{T^4}{\rho}\left[\sum_{\rm ions} Z_j^{\,2}N_j\right]f(\omega_{\rm pl}/T,\kappa_{\rm ions}/T)\ , \quad (21)$$

where

$$\kappa_{\rm ions}^{\,2}=\frac{4\pi\alpha}{T}\sum_{\rm ions} Z_j^{\,2}N_j\ . \quad (22)$$

In Fig. 3 we have plotted the axion emissivity of a pure helium plasma at temperature $T=3\times10^7$ K as a function of density. Curve (a) represents $\epsilon_{\rm nd}$ as in Eq. (13) where the effect of electron degeneracy is ignored throughout, while curve (b) represents $\epsilon_{\rm ions}$ from Eq. (21) in which electrons are assumed to form a uniform background of negative charge throughout. It is apparent that the two curves asymptotically approach each other at high densities, i.e., at strong electron degeneracy. This effect can be understood by observing that at high densities the plasma frequency becomes larger than the temperature such that the blackbody photon spectrum is strongly peaked at energies slightly above, but of the same order as $\omega_{\rm pl}$. Then the parameter s is

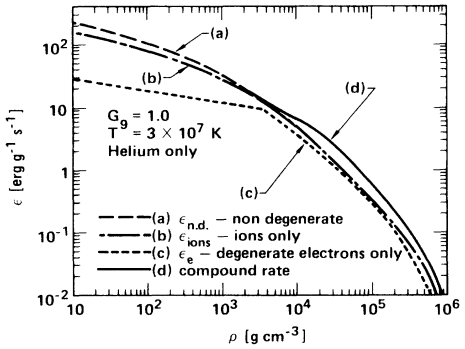

FIG. 3. Energy loss of a stellar plasma due to axion emission. The rates have to be multiplied by $G_9^{\,2}$ in order to obtain the actual losses. Curve (a) is the case for a nondegenerate plasma as given by Eq. (13). Curve (b) is for the case where electrons are treated as a homogeneous background of negative charge as in Eq. (21). Note that curves (a) and (b) merge at degenerate conditions as discussed in the main text. Curve (c) assumes perfect electron degeneracy and treats the ions as a homogeneous background of positive charge. The kink in this curve is due to the approximation Eq. (28). Curve (d) is the compound rate as in Eq. (26). Note that at low densities curve (d) is identical with (a).

$$s=\frac{\kappa^2}{2\omega(\omega^2-\omega_{\rm pl}^{\,2})^{1/2}}\approx\frac{\kappa^2}{\omega_{\rm pl}^{\,2}}\approx\frac{m_e}{T}\gg1\ , \quad (23)$$

where the approximations are valid up to factors of order unity. Therefore, Eq. (19) is a valid approximation. This means that $f(\omega_{\rm pl}/T,\kappa/T)$ approximately depends on κ only through a factor $1/\kappa^2$ which contains a factor $(\sum_j Z_j^{\,2}N_j)^{-1}$ which then cancels against the corresponding factor in front of Eq. (13). Hence for $\omega_{\rm pl}\gg T$ the axion emission rate does not depend on the number densities of various charged-particle species: The reduction of ϵ brought about by the removal of some of the charged particles is exactly compensated for by the corresponding reduction of screening effects for the remaining targets.

Although degenerate electrons are much weaker correlated with the ions of the plasma and with each other, they are not entirely uncorrelated; the relevant length scale being the Thomas-Fermi wave number

$$\kappa_{\rm TF}^{\,2}=4\alpha m_e p_F/\pi\ . \quad (24)$$

This expression is valid only in the nonrelativistic regime. It is derived and its relevance as a screening length scale is discussed, e.g., in Ref. 42. When we argued that degenerate electrons did not contribute to the screening of ions we really meant $\kappa_{\rm TF}\ll\kappa_{\rm ions}$, a condition which precisely characterizes the fact that the electrons are degenerate and cannot be squeezed into an arbitrarily small volume. The electron contribution to the axion emission in the degenerate regime is then approximated by the same procedure as above with some obvious modifications:

$$\epsilon_e=\frac{\alpha G^2}{4\pi}\frac{T^4}{\rho}R_{\rm deg}N_e f(\omega_{\rm pl}/T,\kappa_{\rm TF}/T)\ , \quad (25)$$

where the reduction factor, due to Pauli blocking, has been defined in Eq. (9). In this treatment we have neglected all correlations between electrons and ions. For the ions, we have treated the electrons as an inert uniform background of negative charge, and for the electrons we have treated the ions as a uniform background of positive charge.

It is not at all obvious whether in a regime of strong electron degeneracy the electrons or the ions are the dominant targets for the Primakoff conversion of photons. The electron contribution is enhanced by the reduction of screening effects because $\kappa_{\rm TF}\ll\kappa_{\rm ions}$, but it is reduced by the Pauli blocking of final states, and the tradeoff is not easily estimated. In Fig. 3, curve (c), we have plotted ϵ_e for the same conditions as above. Numerically it turns out, then, that electrons never are of dramatic importance in comparison with ions for conditions relevant to our study, but that under degenerate conditions they contribute almost as much as the ions.

We have made no attempt to calculate ϵ in the intermediate regime of onsetting degeneracy, but rather have taken recourse to an interpolation between the cases of nondegenerate and strongly degenerate conditions. To this end we have used the expression

$$\epsilon=(1-w)\epsilon_{\rm nd}+w(\epsilon_{\rm ions}+\epsilon_e)\ , \quad (26)$$

where w is a weight which we have chosen as a function of the parameter $\zeta=(3\pi^2N_e)^{2/3}/2m_eT$ which at high density approaches the Fermi energy in units of the temperature, $p_F{}^2/2m_eT$. We have arbitrarily chosen

$$w(\zeta)=\frac{1}{\pi}\arctan(\zeta-3)+\tfrac{1}{2}\ , \tag{27}$$

and we have approximated the Pauli-reduction factor as

$$R_{\rm deg}=1.50/\max\ (1.50,\zeta)\ . \tag{28}$$

Curve (d) in Fig. 3 illustrates the compound emission rate.

In constructing this emission rate we have aimed at a maximum deviation from the true value of less than a few tens of percent. The true error, of course, is impossible to assess on the basis of the foregoing discussion. We believe, however, that the emission rate thus constructed is about the best one can do without having to devote a disproportionate amount of effort to this calculation, an effort that would not reflect in the precision or significance of the final result of this study.

IV. EVOLUTION TO THE HELIUM FLASH

We begin our discussion with a brief summary of the major evolutionary stages of stars with masses near $1M_\odot$; for a detailed discussion see Refs. 43 and 44. After such a star has contracted to the zero age main sequence, hydrogen ignites in its center and it spends the major part of its lifetime quietly burning hydrogen to helium. It remains at an almost fixed location in the Hertzsprung-Russell (HR) diagram (see Fig. 4) where we have displayed the evolution of a $1.3M_\odot$ star with a metallicity of $Z=0.02$ and an initial hydrogen abundance of $X=0.73$. We have chosen this composition because it has been pointed out that the stars of M67 are very similar to the Sun and surprisingly homogeneous in composition.[26] After the exhaustion of hydrogen in its center the star moves horizontally away from the main sequence, performing a little "jump" in the HR diagram at the beginning of this phase which observationally corresponds to a gap in the color-magnitude diagram (see Fig. 4 and Ref. 43). Internally this phase of subgiant evolution corresponds to hydrogen burning in a thick shell which is supported by an increasingly degenerate helium core and surrounded by a constantly expanding envelope.

The track in the HR diagram then bends over and the star enters the red-giant branch where the luminosity increases while the surface temperature further decreases. Internally this corresponds to hydrogen burning in a very thin shell. The helium core is now entirely degenerate and practically isothermal. The density profile displays, with good approximation, a step-function behavior and drops within the hydrogen-burning shell from around 10^5 g cm^{-3} in the core to less than 10^{-4} g cm^{-3} in the envelope. During that period the core mass constantly grows and its radius decreases; hence, gravitational energy is released directly in the core and constitutes an important energy source for the heating of the core—not for the overall luminosity of the star.

The core mass keeps growing as the burning front moves outward. It becomes hotter and denser until the triple-α reaction commences. It has a very steep dependence on temperature ($>T^{30}$) and density because it is effectively a three-body reaction. Nuclear burning in a nondegenerate region is self regulating in that an increase in the energy production rate raises the temperature and pressure. This results in expansion, cooling, and reduction of the energy production rate to a steady-

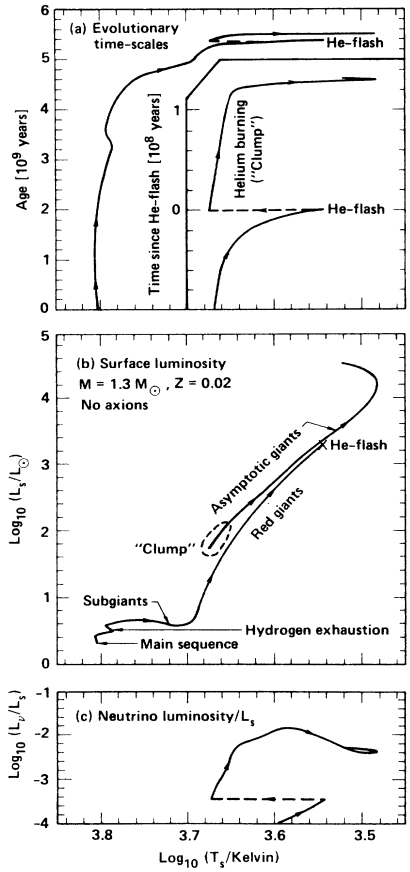

FIG. 4. Evolution of a $1.3M_\odot$ star ($Z=0.02$, $X=0.73$) from zero age to the asymptotic giant branch. No mass loss has been implemented during the red-giant phase. (a) shows age vs surface temperature. (b) is surface luminosity vs surface temperature, i.e., the usual Hertzsprung-Russel diagram. (c) is the ratio of neutrino luminosity (from the interior) over surface luminosity vs surface temperature. At the given arrangement of these figures one can directly read from (a) the time spent in each evolutionary phase shown in (b). It is evident, for example, that the star spends most of its time at the main sequence, the end of which is marked by "hydrogen exhaustion," referring to the center of the star. The inset in (a) gives increased time resolution for the phases immediately before and after the helium flash. It is evident, in particular, that the star spends about 1.2×10^8 yr at the location marked clump in the HR diagram. From (c) it is obvious that at the helium flash the neutrino luminosity decreases by practically the same factor as the surface luminosity (because of the lowered density of the core) so that L_ν/L_s remains virtually constant.

state value. In a star in which degeneracy pressure provides the support, the temperature may increase without an immediate self-regulating response. Therefore, once the energy-generation rate is large enough to balance the neutrino losses, a thermal runaway reaction occurs: The helium flash. Helium typically ignites somewhat off center because neutrino losses are largest in the center of the star [see, e.g., Fig. 7(e)]. The runaway is checked once the core degeneracy has been lifted and the usual self-regulation sets in. Then the star settles in a new equilibrium position with a nondegenerate, helium-burning core and a hydrogen-burning shell. The core mass, surface temperature, luminosity, and age at which the helium flash occurs are given for a $1.3M_\odot$ and for a $1.0M_\odot$ star in the first row of Table III. Our core masses are slightly larger (by about 0.01) but still in good agreement with those derived from Eq. (3) of Ref. 44.

Including the effect of axion cooling as calculated in the previous section we find that the helium flash occurs delayed, depending on the choice of the axion-photon coupling G. For a $1.3M_\odot$ star *it did occur for all values of G which satisfy the solar bound.* For a $1.0M_\odot$ star it was not quite clear whether or not it occurred at $G_9=2.5$ because the numerical solution became quite unstable. For $G_9=1.0$ and below, it unquestionably occurred for both masses. The relevant results are listed in Table III. It is apparent that the core mass and surface properties at the time of the helium flash are quite insensitive to the initial mass of the star. Specifically the maximum luminosity at the top of the giant branch is a rather universal value for a relatively wide range of stellar masses.

In Fig. 5 we display the Hertzsprung-Russell diagram for $G_9=0.3$ and in Fig. 6 for $G_9=2.5$, both for the $1.3M_\odot$ case. We also display the relative luminosity in axions and neutrinos, and for the case of $G_9=2.5$ (Fig. 6) it is apparent that during the main-sequence evolution axion losses are substantially above any other energy-loss mechanism of the star. It is very interesting to observe the dramatic drop in the axion luminosity during the subgiant evolution and beyond: it effectively "switches off" in the core. Even the remaining cooling is strong enough, however, to substantially delay the occurrence of the helium flash. The overall evolutionary time scale is reduced—see Table III for the age at the helium flash. For $G_9=1.0$ and below, the time scale remains practically unchanged from the no-axion case, and in the case of $G_9=0.3$ the HR diagram as displayed in Fig. 5 is virtually indistinguishable from the no-axion case (Fig. 4)—aside from the extension of the giant branch to larger luminosities and the evolution beyond the helium flash.

In Fig. 7 we show the internal structure for a $1.3M_\odot$ star with axion losses at the $G_9=1.0$ level just prior to the helium flash. The axion emission is most dramatic just behind the burning front and strongly decreases toward the center of the core, while for neutrinos the op-

TABLE III. Properties of stars at the helium flash for different values of the axion-photon coupling G. The mass M of the star and the core mass $M_{\rm core}$ at helium flash are in units of the solar mass $M_\odot$. The surface luminosity, temperature, and core radius are understood as logarithms. L_s is in units of $L_\odot$, T_s in degrees Kelvin, $R_{\rm core}$ in centimeters, and the age in 10^9 yr.

G_9	M	L_s	T_s	$M_{\rm core}$	$R_{\rm core}$	Age
0.00	1.0	3.39	3.523	0.489		
	1.3	3.34	3.543	0.477	9.25	5.4
0.10	1.3	3.42	3.534	0.491	9.25	5.3
0.30	1.0	3.66	3.499	0.542		
	1.3	3.68	3.510	0.546	9.21	5.3
1.00	1.0	3.98	3.477	0.644		
	1.3	4.00	3.484	0.648	9.10	4.5
2.50	1.3	4.18	3.474	0.744	9.02	2.1

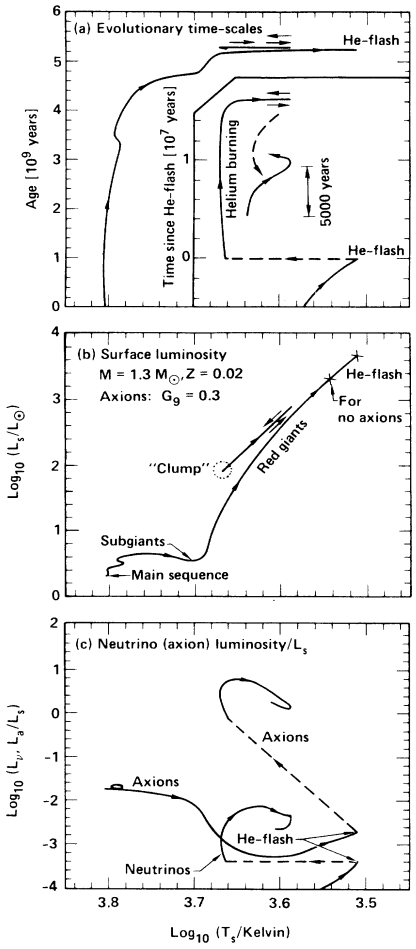

FIG. 5. Evolution of a star as in Fig. 4, now with the inclusion of axions at $G_9=0.3$, about an order of magnitude below the solar bound Eq. (2). The main modification of the HR diagram is the extension of the giant branch to larger luminosities (delayed helium flash) and the dramatic decrease of the helium-burning lifetime. In (c) we also show the relative axion luminosity. It is important to note that at the helium flash it jumps to substantially larger values and becomes the dominant energy-loss mechanism for the star. This is direct evidence that axion losses are most important during the helium-burning phase as anticipated in previous work.

posite is true because they are emitted dominantly through the plasma decay process [Fig. 7(e)]. The temperature profile in the core displays marked differences between the two cases [Figs. 7(b) and 7(c)]. In the neutrino-only case it has a minimum in the center and a maximum somewhere halfway out to the core boundary. For the neutrino-plus-axion case it has a distinct maximum at the burning front, a shallow minimum just behind it, and a maximum at the center of the star. Consequently, the rate for the triple-α reaction is maximum in the center [Fig. 7(e)] such that the helium flash occurs from there. In the neutrino-only case, in contrast, it occurs from a shell off center.

Our computer code uses the "classical" neutrino emission rates of Beaudet, Petrosian, and Salpeter[45] (BPS), although recently, new numerical studies of the emission rates in the standard weak-interaction model have appeared.[46] However, for the conditions of interest in our discussion, the plasmon decay emissivity dominates. Because of the peculiar value $\sin^2\Theta_w \approx \frac{1}{4}$ of the weak mixing angle, the electron neutral current is almost entirely axial so that the plasmon decay rate remains virtually unchanged from the BPS results.

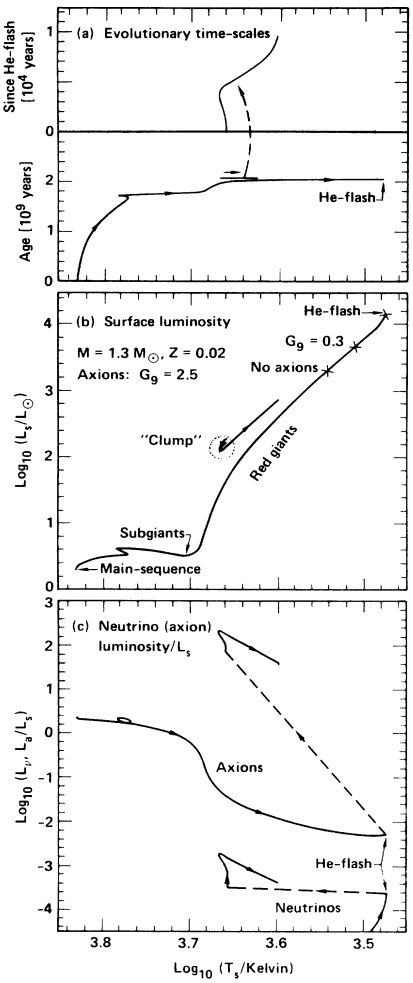

FIG. 6. Evolution of a star as in Figs. 4 and 5, with axions now at $G_9 = 2.5$ which just saturates the solar bound Eq. (2). The changes brought about by axion cooling are similar as in Fig. 5, but now even the main-sequence lifetime is substantially reduced.

The luminosity as a function of the radial mass coordinate is in some regions within the core *negative,* implying *inward* energy flow—see the dashed parts of the curves in Fig. 7(d). Considering the situation just prior to the helium flash, it is apparent that in the neutrino-plus-axions case a substantial heat flow from the burning front into the core exists. It is stopped, however, by excessive axion emission such that the core can be thought of as being thermally isolated from the burning shell. An outward heat flow from the center where no net energy generation takes place also exists. The triple-α reaction is still far below neutrino plus axion losses [Fig. 7(e)]. The center of the star, however, slowly heats; a fact which emphasizes the importance of gravitational energy as a heat source for the core.

The effect of gravitational energy release is also illustrated by the values for the core radii at helium flash in Table III: They *shrink* with rising values for the core masses (associated with larger values of G)—a well-known behavior for the mass-radius relationship of degenerate stars.[42] It indicates that substantial amounts of gravitational binding energy are released which heat the core unless the cooling by neutrinos and other particles is efficient enough to balance this effect.

Our results allow to set interesting bounds on G because of the increased surface luminosity at the top of the giant branch. For $G_9 = 0.3$ the luminosity at the helium flash is increased by $\Delta\log_{10}(L/L_\odot) = 0.34$, corresponding to an increase in luminosity by more than a factor of 2, or, in astronomical units, to a decrease of the magnitude (increase in brightness) of $\Delta m = -2.5\Delta\log_{10}(L/L_\odot) \approx -0.8$. In all open clusters, stars are observed near the theoretically expected locus of the giant branch in the color-magnitude diagram,[29] and in some cases, up to the expected top of the giant branch, but no stars are ever seen in the range corresponding to the "axion-induced" extension of the giant branch. Even in view of all the uncertainties involved in translating the observational photometric quantities into absolute surface temperatures and luminosities, it appears that a discrepancy of Δm on the order of unity would be too large to be absorbed in these errors. Therefore, we argue that the observational absence of an anomalous extension of the giant branch establishes the bound $G_9 \lesssim 0.3$.

Unfortunately, this argument suffers from the statistical uncertainty inherent in the small number of stars populating the giant branch in open clusters (typically a few tens of stars). It is therefore, perhaps, not entirely excluded that the observational absence of stars in an extended giant branch is just a statistical small-number effect. This uncertainty would not pertain to the case of globular clusters which typically are much more populous than open clusters. There, too, a sharp cutoff at the top of the giant branch is observed, supporting our argument for the case of open clusters. We concede that, in order to make our present argument absolutely unrefut-

able, we would have to go through the same numerical procedure as before for the case of less massive, metal-poor stars typical for globular clusters (Population II stars). Since a much more interesting bound can be obtained, however, from the helium-burning lifetimes of our present stellar models, we proceed to consider the evolution beyond the helium flash.

V. HELIUM-BURNING PHASE

Considering the helium-burning phase we mention that it is very difficult to follow the helium flash numerically. Calculations of Härm and Schwarzschild[47] of this phase found a hydrostatic expansion of the core followed by the establishment of a core helium-burning configuration. This expansion is very quick and the preflash composition profile of the star is maintained during this process. We have expanded the core of our preflash models "by hand" to this position in order to avoid the numerical difficulties of following the helium flash. More recent hydrodynamic models of Deupree and Cole[48] have found a range of possible behaviors during the helium flash. Depending on the initial helium core model they can closely resemble the behavior found in the hydrostatic calculations or, on the other side of the spectrum of possible behaviors, they can show complete mixing and a second main-sequence phase. We believe that the observed chemical composition of the clump giants[26,49] indicates that most stars expand in the hydrostatic manner. We have neglected the possibility of mass loss and have chosen a total mass of $1.3M_{\odot}$, a metallicity $Z=0.02$, and core masses according to the values listed in Table III for our "zero age" helium-burning stars. We then follow their evolution with the strength of axion cooling appropriate for the different core masses.

For the no-axion case the relevant evolution is shown

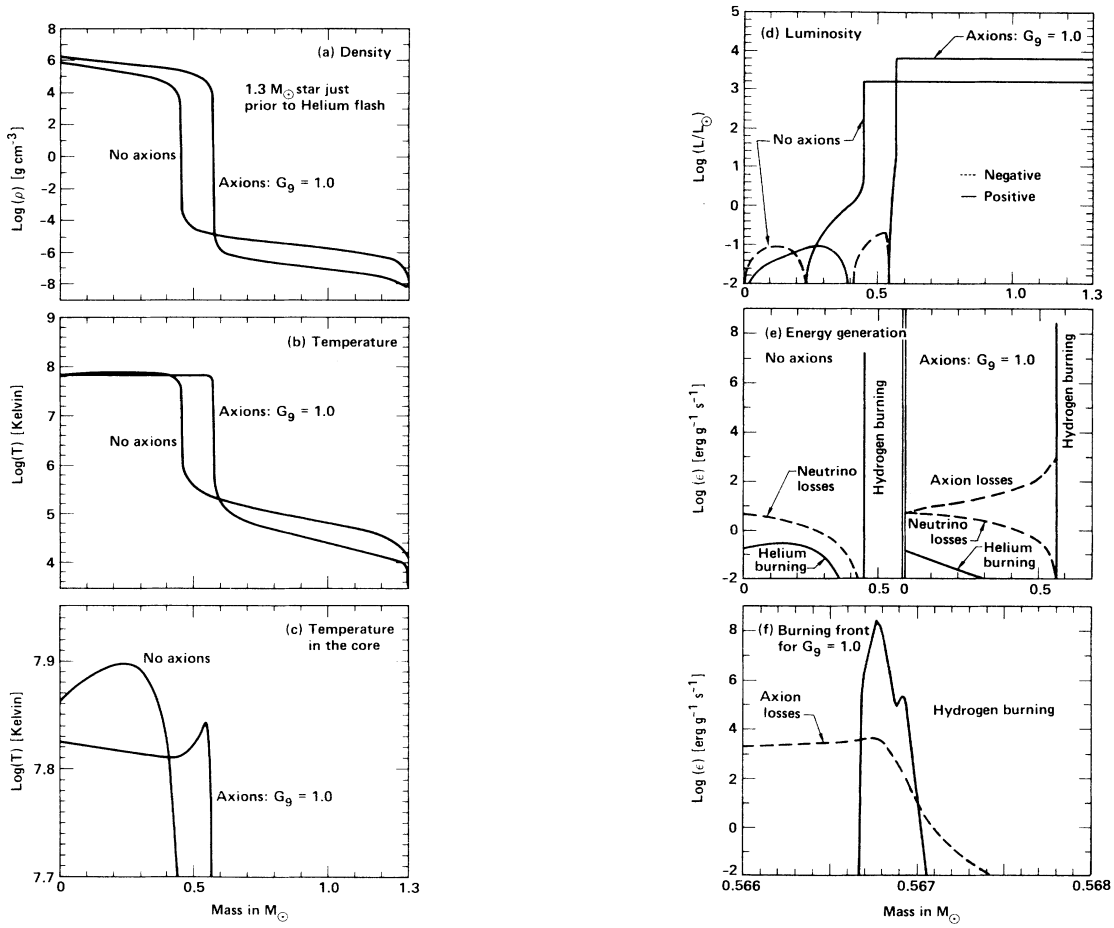

FIG. 7. Internal structure of a $1.3M_{\odot}$ star ($X=0.73$, $Z=0.02$) just prior to the helium flash, with and without axion emission. "Just prior" means that helium-burning commences, but still is of only minor importance and, in particular, far below the neutrino and axion losses. It is noticeable, however, that for no axions the flash will take place from a shell off center, while for axions at the given interaction strength of $G_9=1.0$ it will take place from the center. This is confirmed by later models of these stars. Note that in both cases the core will grow considerably before the helium flash actually occurs, so that the present core masses are well below the values given in Table III. In (d) the dashed parts of the curves refer to *negative* values of L (which are difficult to plot on a logarithmic scale) and which refer to *inward* heat flow. In (e) the dashed curves refer to energy losses (axions, neutrinos), while the solid curves refer to (nuclear) energy generation. For other details see the discussion in the main text.

in Fig. 4: The star spends a little more than 10^8 yr at an almost fixed location in the HR diagram, quietly burning helium in its center and hydrogen in a shell. After the exhaustion of helium in its center, it quickly moves up the asymptotic giant branch, with a much faster time scale than the helium-burning lifetime and also much faster than the giant branch evolution. This implies that many stars should be observable at the location in the HR diagram labeled clump in Fig. 4(b). This clump of giant stars is indeed observed in all open clusters.[27]

Implementing axion cooling at the $G_9=0.3$ level, far below the solar bound, substantially alters this picture. In this context we emphasize the important difference between the neutrino and the axion track in Fig. 5(c): The neutrino luminosity drops dramatically after the helium flash because of the much reduced core density so that the ratio L_ν/L_s remains virtually constant, while for axions the opposite effect occurs. This underscores the fact that axion emission is most dramatic in the helium-burning phase of stars. The time scale for this phase is now reduced by about an order of magnitude (see Table IV) so that one would expect only a tenth of the standard number of clump stars to be observable in open clusters. On the asymptotic giant branch, the star reaches a maximum luminosity very quickly and then reverses its track.

We emphasize that a reduction of the number of clump giants by an order of magnitude would render the clump entirely unobservable in most or all open clusters because it consists only of a small number of stars to begin with,[27] e.g., 4 in NGC 752, 5 in M67, 20 in NGC 6939, and 41 in NGC 7789. Therefore our previous bound $G_9 \lesssim 0.3$ is confirmed in an extremely conservative manner.

We believe that one can do substantially better by comparing the total number of clump giants with the number of other stars (particularly near the turn-off point on the main sequence) in the cluster. As previously stressed, the time scale for the phases preceding helium-burning remain virtually unchanged for $G_9=1.0$ and below, while the helium-burning lifetime is substantially reduced. This behavior becomes particularly graphic by comparing Fig. 4(a) with Fig. 5(a), and is also indicated by the entries in the last column of Tables III and IV. Therefore, the axion cooling effect would directly affect the *ratio* of the number of clump giants versus stars in any previous evolutionary phase.

From star counts in the cluster M67 Cannon[27] derives a clump lifetime of $t_{\rm He}=1.5\times10^8$ yr with a statistical $\sqrt{N}$ uncertainty of about 50% because of the small number of clump giants, $N=5$. Tinsley and Gunn[30] derive $t_{\rm He}=(1.27\pm0.29)\times10^8$ yr from low mass giants of the old galactic disk population. Our result of $t_{\rm He}=1.2\times10^8$ yr for the no-axion case is in very satisfactory agreement with these numbers. We mention that Cannon similarly derives for M67 a time scale 6×10^8 yr for the red-giant lifetime, excluding the clump and the subgiant phase. In contrast to the clump, this latter giant sequence is not entirely well defined theoretically in that it is not obvious where precisely the line between subgiants and giants should be drawn. Therefore, we derive from our calculation for the no-axion case, a somewhat uncertain giant branch lifetime of $4-5\times10^8$ yr, a number which again is in very good agreement with Cannon's result and underscores the reliability of the calculation.

TABLE IV. Time scale for helium burning for a $1.3M_\odot$ star for various values of G.

G_9	$t_{\rm He}$ (yr)
0.0	1.2×10^8
0.1	6.9×10^7
0.3	1.6×10^7

We believe that in view of the impressive agreement of observations with calculations for the no-axion case, a reduction of the helium-burning lifetime by a factor of 2 is, at best, marginally consistent with the observational data. We therefore argue that $G_9 \lesssim 0.1$, corresponding with Eq. (3) to $m_a \lesssim 0.7$ eV R, is a reasonably safe upper bound. We mention that even an uncertainty in our calculations of the axion emission rates of a factor 2 would relax these bounds only by a factor $\sqrt{2}$.

These limits are numerically similar to the bound offered in paper II, but we emphasize that our present result is directly linked to observational data which is the major improvement over previous work.

VI. CONCLUSIONS

We have considered in detail the effect of hadronic axion cooling on stellar evolution. To this end we have confirmed the solar bound Eq. (2) $G \lesssim 2.5\times10^{-9}$ GeV^{-1} ($m_a \lesssim 17$ eV R) from the evolution of $1.0M_\odot$ stars to solar age and adjusting the presolar helium abundance Y such as to achieve consistency with the observed solar luminosity. The effect of axion cooling is to *decrease* the inferred value of Y, a result that cannot easily be excluded from observational evidence which, on the contrary, possibly favors a lower value for Y than is obtained from standard solar models.

In order to follow the evolution of stars up the giant branch to the helium flash, we have constructed new Primakoff emission rates for a stellar plasma and have attempted to take plasma, degeneracy, and screening effects properly into account because of the large variety of conditions encountered in a giant star. The emission rates are strongly suppressed at high densities. In the post-main-sequence evolution, and particularly on the giant branch, this manifests itself as an effective switch off in the stellar core of axion emission although the residual effect is strong enough to delay the occurrence of helium ignition.

The main reason for the actual occurrence of the helium flash for all values of the axion-photon coupling permitted by the above solar bound is the excessive release of gravitational energy in the core which grows in mass beyond its standard value, but shrinks in size. Helium ignition can only be suppressed by an exotic cooling mechanism if it is efficient enough to shield the core from the hydrogen-burning front and balance the release

of gravitational energy in the core.

The helium flash occurs, however, at a much increased surface luminosity. The requirement that it not be increased by more than a factor of 2—which would be in disagreement with observational evidence concerning the luminosity at the top of the giant branch in open clusters—translates into a bound of $G \lesssim 0.3 \times 10^{-9}$ GeV^{-1} ($m_a \lesssim 2$ eV R). This bound is statistically somewhat uncertain because of the small number of stars on the giant branch in open clusters. This argument could be improved by considering Population II stars typical for globular clusters which are generically much more populous than open clusters.

Our strongest bound is obtained from star counts in the open cluster M67 and the old galactic disk population which can be translated into lifetimes of clump giants. The impressive agreement between these observational numbers and our calculated helium-burning time scale for the no-axion case establishes the bound

$$G \lesssim 10^{-10}\ \mathrm{GeV}^{-1}\ . \tag{29}$$

If this bound were saturated a severe conflict between observations and calculations would occur.

We conclude that the detection of cosmic axions through their 2γ decay as envisaged by Kephart and Weiler and by Turner[16] is excluded. The influence of axion cooling on the Sun would be very small. From paper II we find that the flux of axions from the Sun, for which now a standard model can be assumed, is $L_a \approx 0.17 G_9^2 L_\odot$ so that $L_a < 0.002 L_\odot$ for $G_9 < 0.1$. The maximum of the axion spectrum would be at 4–5 keV, much in excess of the internal temperature of the Sun (see paper II). It is not obvious whether a recently proposed detector[50] for the solar axion flux could operate at this low flux level and below. Recently several laboratory experiments have been suggested which would be sensitive to the axion-photon coupling. In these experiments a laser beam would be propagated through an external magnetic field, and axions could be detected by either measuring the changes in the polarization state of the beam,[51] or else by "shining light through walls."[52] There remains a narrow window of parameters ($0.01 \lesssim G_9 \lesssim 0.1$, $m_a \lesssim 10^{-4}$ eV) in which these experiments might be sensitive and which is not excluded by our bounds.

Besides the new bounds on hadronic axions provided by our work, we hope to have contributed to a better understanding of the method of using stellar evolution as a probe for particle physics. We are confident that this knowledge will prove useful in other cases besides the specific problem discussed here.

ACKNOWLEDGMENTS

We thank Ch. Alcock, H.-Y. Cheng, D. Seckel, J. Silk, and T. Weiler for discussions and comments. At Berkeley, this work was supported, in part, by NASA and DOE. At Livermore, this work was performed under the auspices of the U.S. Department of Energy under Contract No. W-7405-ENG-48.

[1]R. D. Peccei and H. Quinn, Phys. Rev. Lett. **38**, 1440 (1977); Phys. Rev. D **16**, 1791 (1977). For a recent review of the *CP* problem and the Peccei-Quinn mechanism, see H.-Y. Cheng, Phys. Rep. (to be published).

[2]S. Weinberg, Phys. Rev. Lett. **40**, 223 (1978); F. Wilczek, *ibid.* **40**, 279 (1978).

[3]R. D. Peccei, in *Grand Unified Theories and Related Topics*, proceedings of the Fourth Kyoto Summer Institute, Kyoto, Japan, 1981, edited by M. Konuma and T. Maskawa (World Scientific, Singapore, 1981).

[4]R. D. Peccei, T. T. Wu, and T. Yanagida, Phys. Lett. B **172**, 435 (1986); L. M. Krauss and F. Wilczek, *ibid.* **173**, 189 (1986).

[5]For short-lived axions, see T. Bowcock *et al.*, Phys. Rev. Lett. **56**, 2676 (1986); A. L. Hallin, F. P. Calaprice, R. W. Dunford, and A. B. McDonald, *ibid.* **57**, 2105 (1986); C. M. Hoffman, Phys. Rev. D **34**, 2167 (1986); G. Mageras *et al.*, Phys. Rev. Lett. **56**, 2672 (1986).

[6]For general properties of invisible-axion models and for references to the original literature, see D. B. Kaplan, Nucl. Phys. **B260**, 215 (1985); M. Srednicki, *ibid.* **B260**, 689 (1985).

[7]J. Preskill, M. B. Wise, and F. Wilczek, Phys. Lett. **120B**, 127 (1983); L. F. Abbott and P. Sikivie, *ibid.* **120B**, 133 (1983); M. Dine and W. Fischler, *ibid.* **120B**, 137 (1983); W. G. Unruh and R. M. Wald, Phys. Rev. D **32**, 831 (1985); M. S. Turner, *ibid.* **32**, 843 (1985). This bound, however, has a very peculiar status as emphasized by R. L. Davis, Phys. Lett. B **180**, 225 (1986): If inflation occurs in the early Universe and if reheating remains below v_{PQ}, this bound depends on the assumption that the initial value of the axion field is of order v_{PQ}. If no inflation occurs or if $T_{\mathrm{reheat}} > v_{PQ}$, the formation and subsequent decay of axionic strings would produce many axions, and then, according to Davis, $v_{PQ} \lesssim 10^{10}\ \mathrm{GeV}^{-1}$.

[8]M. S. Turner, Phys. Rev. D **33**, 889 (1986).

[9]P. Sikivie, Phys. Rev. Lett. **51**, 1415 (1983); **52**, 695(E) (1984); Phys. Rev. D **32**, 2988 (1985).

[10]S. DePanfilis *et al.*, Phys. Rev. Lett. **59**, 839 (1987).

[11]This model is usually referred to as the DFS model after M. Dine, W. Fischler, and M. Srednicki, Phys. Lett. **104B**, 199 (1981), but it was first proposed by A. R. Zhitnitsky, Yad. Fiz. **31**, 260 (1980) [Sov. J. Nucl. Phys. **31**, 260 (1980)]. Following Cheng (Ref. 1) we propose the term "DFSZ model." For an overview, see Cheng (Ref. 1) and Ref. 6.

[12]J. Kim, Phys. Rev. Lett. **43**, 103 (1979); M. A. Shifman, A. I. Vainshtein, and V. I. Zakharov, Nucl. Phys. **B166**, 493 (1980). See also Ref. 6.

[13]G. G. Raffelt, Phys. Lett. **166B**, 402 (1986).

[14]D. S. P. Dearborn, D. N. Schramm, and G. Steigman, Phys. Rev. Lett. **56**, 26 (1986), hereafter denoted as paper I.

[15]G. G. Raffelt, Phys. Rev. D **33**, 897 (1986), hereafter denoted as paper II. In this work detailed references to previous studies of the question of axion emission from stellar bodies are given.

[16]T. W. Kephart and T. J. Weiler, Phys. Rev. Lett. **58**, 171 (1987), where only the coherent axion production mechanism

has been considered. It was then shown by M. S. Turner, Report No. Fermilab-Pub-86/150-A, 1986 (unpublished), that the Primakoff production would dominate in the relevant parameter range so that the number of relic axions is larger than originally thought. Both groups of authors have neglected axion production through decay of axionic strings (see Ref. 7). We find, however, that even then, Primakoff production remains the dominant mechanism in the range $m_a \gtrsim 1$ eV, taking $R=1$. Therefore, Turner's results are quite independent of specific assumptions concerning the very early Universe.

[17]N. Iwamoto, Phys. Rev. Lett. **53**, 1198 (1984).

[18]A. Pantziris and K. Kang, Phys. Rev. D **33**, 3509 (1986). For a comment on this work see Ref. 41.

[19]S. Tsuruta and K. Nomoto, Observational Cosmology, proceedings of the IAU Symposium No. 24, Beijing, 1986 (to be published); S. Tsuruta (private communication).

[20]D. E. Morris, Phys. Rev. D **34**, 843 (1986).

[21]G. G. Raffelt and L. Stodolsky, Report No. MPI PAE/PTh 54/87, 1987 (unpublished).

[22]E. Witten, Phys. Rev. D **30**, 272 (1984).

[23]See, e.g., C. Alcock, E. Farhi, and A. Olinto, Astrophys. J. **310**, 261 (1986).

[24]L. Stodolsky, J. Phys. (Paris) Colloq. **35**, C2-87 (1974).

[25]O. J. Eggen and A. R. Sandage, Astrophys. J. **140**, 130 (1964); R. Racine, *ibid.* **168**, 393 (1971).

[26]K. A. Janes and G. H. Smith, Astron. J. **89**, 487 (1984).

[27]R. D. Cannon, Mon. Not. R. Astron. Soc. **150**, 111 (1970).

[28]D. J. Faulkner and R. D. Cannon, Astrophys. J. **180**, 435 (1973).

[29]R. G. Gratton, Astrophys. J. **257**, 640 (1982).

[30]B. M. Tinsley and J. E. Gunn, Astrophys. J. **206**, 525 (1976).

[31]F. T. Avignone, R. L. Brodzinski, H. S. Miley, and J. H. Reeves, Report, 1987 (unpublished). For the opposite conclusion, see D. O. Caldwell, R. M. Eisberg, D. M. Grumm, and M. S. Witherell, report, 1987 (unpublished).

[32]L. M. Krauss, J. E. Moody, and F. Wilczek, Phys. Lett. **144B**, 391 (1984).

[33]M. Nakagawa, Y. Kohyama, and N. Itoh, Astrophys. J. (to be publsihed).

[34]L. Wolfenstein, Phys. Rev. D **17**, 2369 (1978); **20**, 2634 (1979); S. P. Mikheyev, A. Yu. Smirnov, Yad. Fiz. **42**, 1441 (1985) [Sov. J. Nucl. Phys. **42**, 913 (1985)]; Nuovo Cimento **9C**, 17 (1986); Zh. Eksp. Teor. Fiz. **91**, 7 (1986) [Sov. Phys. JETP **64**, 4 (1986)]; H. A. Bethe, Phys. Rev. Lett. **56**, 1305 (1986).

[35]R. L. Sears, Astrophys. J. **140**, 477 (1964).

[36]J. N. Bahcall, W. F. Huebner, S. H. Lubow, P. D. Parker, and R. K. Ulrich, Rev. Mod. Phys. **54**, 767 (1982).

[37]M. Cassé, S. Cahen, and C. Doom, in *Neutrinos and the Present-Day Universe,* edited by Th. Montmerie and M. Spiro (Editions Frontières, Saclay, Gif-sur-Yvette, 1986).

[38]D. S. P. Dearborn and G. Fuller, Report, 1987 (unpublished).

[39]G. J. Ferland, Astrophys. J. **310**, L67 (1986).

[40]For a review, see M. Baus and J.-P. Hansen, Phys. Rep. **59**, 1 (1980).

[41]For a brief discussion of some aspects of stimulation effects in the context of stellar axion emission, see G. G. Raffelt, Phys. Rev. D **34**, 3927 (1986).

[42]S. L. Shapiro and S. A. Teukolsky, *Black Holes, White Dwarfs, and Neutron Stars—The Physics of Compact Objects* (Wiley, New York, 1983).

[43]I. Iben, Jr., Astrophys. J. **147**, 624 (1967).

[44]I. Iben and A. Renzini, Phys. Rep. **105**, 329 (1984).

[45]G. Beaudet, V. Petrosian, and E. E. Salpeter, Astrophys. J. **150**, 979 (1967).

[46]H. Munakata, Y. Kohyama, and N. Itoh, Astrophys. J. **296**, 197 (1985); **304**, 580(E) (1986), and references therein; P. J. Schinder, D. N. Schramm, P. J. Wiita, S. H. Margolis, and D. L. Tubbs, Report No. Fermilab-Pub-86/100-A, 1986 (unpublished).

[47]R. Härm and M. Schwartzschild, Astrophys. J. **139**, 594 (1964); **145**, 496 (1966).

[48]R. G. Deupree and P. W. Cole, Astrophys. J. **269**, 676 (1983).

[49]G. H. Smith and J. Norris, Astron. J. **89**, 263 (1984).

[50]D. E. Morris (private communication).

[51]L. Maiani, R. Petronzio, and E. Zavattini, Phys. Lett. B **175**, 359 (1986). This work, unfortunately, overestimates the axion effect, see Ref. 21.

[52]K. van Bibber *et al.*, Phys. Rev. Lett. **59**, 759 (1987); M. Gasperini, *ibid.* **59**, 396 (1987).